Polarization and Polarization Transfer in the Reaction $T(p,n)^3He$†

R. C. Haight, J. E. Simmons
Los Alamos Scientific Laboratory, University of California, Los Alamos, New Mexico 87544

and

T. R. Donoghue*
Los Alamos Scientific Laboratory, University of California, Los Alamos, New Mexico 87544, and Ohio State University, Columbus, Ohio 43210

(Received 27 December 1971)

The polarization-transfer coefficients $K_y^y(\theta)$, $K_x^{x'}(\theta)$, and $K_z^{x'}(\theta)$ in the reaction $T(p,n)^3He$ have been measured for seven laboratory angles between 15 and 120° at $E_p = 13.55$ MeV. At $E_p = 8.94$ MeV, $K_x^{x'}(30°)$ and $K_z^{x'}(30°)$ were determined. In addition, the polarization function, $P(\theta)$, was measured at 13.55 MeV. The previously reported polarization-transfer data at 0° as a function of energy are given here in more detail. Comparisons are made with R-matrix calculations based on the analysis of Werntz and Meyerhof.

I. INTRODUCTION

A recent study[1] of polarization transfer at 0° in the reaction $T(p,n)^3He$ provided new information on the spin dependence of this charge-exchange reaction. The data were compared with calculations based on the charge-independent R-matrix parameters of Werntz and Meyerhof[2] (also referred to as WM) and it was found that neither of their two parameter sets was able to account very well for this new observable. Since the poles of the R matrix are often interpreted as unbound levels of the compound nucleus, some modification was therefore indicated in the experimental level structure of ^4He.

This paper is concerned with an extension of the previous data in the reaction $T(p,n)^3He$ at 0° to angular distributions of the polarization-transfer functions. The chief objective was to accumulate new data relating to the spin-dependent amplitudes for this process. Such data will be used directly in the R-matrix analysis of the four-body problem by Dodder and Hale[3] of this laboratory. Further comparisons also become possible with the WM analysis, which was directly concerned with the $T(p,n)^3He$ process.

We chose $E_p = 13.55$ MeV as the laboratory bombarding energy for the majority of the measurements for several reasons, in spite of the fact that it was somewhat high for best comparisons with WM. First a considerable amount of precise data has been accumulated at 13.60 MeV on the $T+p$ system by Detch *et al.*[4] In addition, this energy allows good beams to be extracted from the tandem accelerator, and is better than lower energies in that the magnitude of multiple-scattering corrections in the liquid-helium polarimeter decreases with increasing neutron energy.

Relatively few other measurements of this kind have been made on low-energy (p,n) reactions. To our knowledge the only prior work in this category is that of Robertson *et al.*[5] They made polarization-transfer measurements at 0° for the reactions $D(p,n)2p$, $^6Li(p,n)^6Be$, and $^7Li(p,n)^7Be$ at 30 and 50 MeV. The polarization-transfer coefficients measured were relatively small in magnitude. The larger effects were of negative sign in the $p+D$ process, which presumably is a manifestation of the p-n quasifree scattering.

For completeness, the results of the previously reported $K_y^y(0°)$ measurements for the $T(p,n)^3He$ reaction are presented in tabular form. The large values noted for this parameter imply that this reaction is an excellent source of polarized neutrons.

II. FORMALISM

The $T(p,n)^3He$ reaction has a spin structure formed of two spin-$\frac{1}{2}$ particles each in the initial and in the final states. In this respect, it is comparable to the nucleon-nucleon (N-N) problem with the exception that symmetries arising from charge independence and time reversal are absent. In this section we review briefly the geometry of the reaction and pertinent aspects of the spin formalism.

The laboratory scattering geometry is shown in Fig. 1. We make use of two frames of reference; the incident laboratory frame is defined by the orthonormal basis $\hat{x}$, $\hat{y}$, $\hat{z}$ while the final or scattered frame is described by the orthonormal ba-

sis $\hat{x}'$, $\hat{y}'$, $\hat{z}'$. The two frames have a common y axis $\hat{y}'=\hat{y}=\hat{n}$, where $\hat{n}$ is the normal to the scattering plane defined by $\hat{n}=\vec{k}_i\times\vec{k}_f/|\vec{k}_i\times\vec{k}_f|$, where $\vec{k}_i$ and $\vec{k}_f$ are the incident and final directions of motion of the nucleons in the laboratory system. The axes $\hat{z}$ and $\hat{z}'$ are taken along $\vec{k}_i$ and $\vec{k}_f$, respectively. For these experiments the reaction plane was the horizontal plane.

The relationship between incident and final polarization vectors was given by Wolfenstein[6] for the case of N-N triple scattering. His formulas apply equally well to the present case which we describe as transfer of polarization from the incident proton to the outgoing neutron. Let the polarization vector of the incident proton beam be described by $\vec{p}_i=(p_{ix},p_{iy},p_{iz})$, and similarly let the polarization of the final neutron flux at the laboratory angle θ be denoted by $\vec{p}_f=(p_{fx'},p_{fy'},p_{fz'})$. The final polarization is related to the incident polarization by the Wolfenstein equations, which read in a somewhat different notation:

$$I(\theta)p_{fx'}=I_0(\theta)[p_{ix}K_x^{x'}(\theta)+p_{iz}K_z^{x'}(\theta)], \tag{1}$$

$$I(\theta)p_{fy}=I_0(\theta)[P(\theta)+p_{iy}K_y^{y}(\theta)], \tag{2}$$

$$I(\theta)p_{fz'}=I_0(\theta)[p_{ix}K_x^{z'}(\theta)+p_{iz}K_z^{z'}(\theta)], \tag{3}$$

with

$$I(\theta)=I_0(\theta)[1+p_{iy}A(\theta)]. \tag{4}$$

In these formulas the following definitions hold: θ is the laboratory angle[7] of the neutron, $I(\theta)$ and $I_0(\theta)$ are the polarized and unpolarized differential cross sections, respectively, $P(\theta)$ is the polarization function, and $A(\theta)$ is the analyzing power. The functions $K_x^{z'}(\theta)$, etc., represent transfer of polarization from the incident proton component (lower index) to the final neutron component (upper index). This notation is modeled after that of Schumacher and Bethe.[8] An attempt is being made here to achieve a more rational notation for these processes and one that is consistent with the Madison convention.[9] The parameters K_y^y, $K_x^{x'}$, $K_z^{x'}$, $K_x^{z'}$, and $K_z^{z'}$ are directly analogous to the triple-scattering parameters of Wolfenstein D, R, A, R', and A', respectively. Further discussion is given in Appendix A justifying the use of the Wolfenstein equations of the N-N problem in the reaction $T(p,n)^3He$.

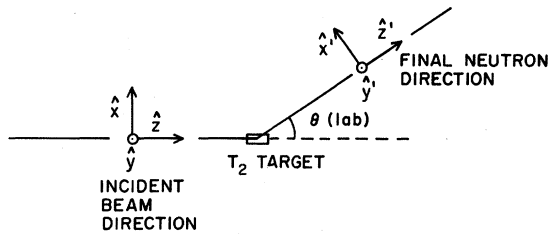

FIG. 1. Illustration of laboratory coordinate systems. The initial frame of reference is defined by the orthonormal basis $\hat{x}$, $\hat{y}$, $\hat{z}$; the final frame of reference is similarly defined by $\hat{x}'$, $\hat{y}'$, $\hat{z}'$, with $\hat{y}=\hat{y}'$.

The various spin-polarization observables of the reaction $T(p,n)^3He$ may be related to the reaction amplitude through the M matrix. MacGregor, Moravcsik, and Stapp[10] have given the general form which is applicable to our cases (see also Appendixes B and C). M is assumed to be a function of the c.m. scattering angle, and incident energy, such that the operations given below yield the polarization-transfer coefficients at the corresponding angle in the laboratory system. The definitions of interest here are the following:

$$K_y^y(\theta)=\mathrm{Tr}(M\sigma_{iy}M^\dagger\sigma_{fy})/\mathrm{Tr}MM^\dagger, \tag{5}$$

$$K_x^{x'}(\theta)=[\cos\theta\,\mathrm{Tr}(M\sigma_{ix'}M^\dagger\sigma_{fx'})+\sin\theta\,\mathrm{Tr}(M\sigma_{iz'}M^\dagger\sigma_{fx'})]/\mathrm{Tr}MM^\dagger, \tag{6}$$

$$K_z^{x'}(\theta)=[-\sin\theta\,\mathrm{Tr}(M\sigma_{ix'}M^\dagger\sigma_{fx'})+\cos\theta\,\mathrm{Tr}(M\sigma_{iz'}M^\dagger\sigma_{fx'})]/\mathrm{Tr}MM^\dagger. \tag{7}$$

The σ's here are the usual Pauli matrices. As is noted in Appendix C, the sine and cosine components arise in expressing the incident polarization vector in the final laboratory frame of reference. The polarization function and the analyzing power also appear in Eqs. (2) and (4), and their definitions in terms of the M matrix are

$$P(\theta)=\mathrm{Tr}(MM^\dagger\sigma_{fy})/\mathrm{Tr}MM^\dagger, \tag{8}$$

$$A(\theta)=\mathrm{Tr}(M\sigma_{iy}M^\dagger)/\mathrm{Tr}MM^\dagger. \tag{9}$$

III. EXPERIMENTAL PROCEDURE

The Los Alamos Lamb-shift polarized ion source[11] produced the polarized proton beam which was accelerated by an FN tandem accelerator. Beam currents on target averaged 96 nA with average polarization of 0.89 for the polarization-transfer runs at 13.55 MeV. The improvement in intensity was due partly to increased output of the source and partly to good transmission through the tandem accelerator. The magnitude of proton polarization was determined by an atomic-beam technique[12] which for the present experiment is believed accurate to ±1.5%. The direction of this polarization was controlled at the source by a spin precessor; however, complete reversal of the spin direction was accomplished by reversing the fields in the spin filter and argon cell described in Ref. 11.

Other experimental details and data-collecting procedures have been described at length elsewhere.[13] The modifications used in these measurements and a brief summary of the method are

as follows: The proton beam impinged on a 3-cm-long tritium gas target maintained at 4.8 absolute atm. The entrance window was a 9.8-mg/cm^2 molybdenum foil plated with 2.4 mg/cm^2 nickel so that it could be soft-soldered to the target cell. The beam was stopped by 0.48 mm of gold which also served as the end wall of the tritium cell.

The polarization of the outgoing neutrons was determined by scattering them in a helium polarimeter which consisted of a 4.8-mole liquid-helium scintillator, denoted as S1, operated in fast coincidence with either of two NE-102 plastic scintillators, denoted as S2 and S3. Accidental coincidences were determined concurrently and were later subtracted from the spectra. The liquid-helium scintillator subtended an angle of $\Delta\theta = 2.08°$ which was the full angular spread over which these measurements were averaged. The dimensions of S2 and S3 were 5.1 cm in $\Delta\theta$ by 19 cm in $\Delta\phi$. The plastic scintillators were positioned above and below the helium sample at n-α scattering angles of 115°. Associated with the polarimeter was a spin-precession solenoid. When the solenoid was off, the polarimeter measured the x' component of polarization of the neutron. The solenoid could also be energized such that the neutron's spin was rotated by ±90° about the z' axis. The y component could thereby be rotated to the horizontal plane and measured. Details of the polarimeter were given in Ref. 13 with the modification that $R_1 = 99$ cm and $R_2 = R_3 = 30$ cm.

For each of the polarization parameters an asymmetry e was measured. Aside from correction factors, e is related to p_f, which is either the final x' component of neutron polarization or the final y component, by

$$e = p_f P(n\text{-}\alpha, 115°), \tag{10}$$

where $P(n\text{-}\alpha, 115°)$ is the n-α analyzing power at 115°.

Experimentally, e is determined from the usual expression $e = (N_+ - N_-)/(N_+ + N_-)$, where N_+ and N_- represent true signal events. For measurement of p_{fy} the asymmetry was obtained by precessing the outgoing neutron spin into the $+x'$ direction to give N_+, and into the $-x'$ direction to give N_-. For measurement of $p_{fx'}$ the asymmetry was obtained by reversing the incident beam polarization, $\vec{p}_i$, with the spin-precession solenoid off. In the case of $K_x^{x'}$, for example, Eq. (1) explicitly shows that $p_{fx'}$ is reversed when $\vec{p}_i$ is reversed. The quantities N_+ and N_- therefore correspond directly to opposite signs of outgoing neutron polarization. In all measurements, cycles of $+--+$ were performed to reduce the effects of electronic drifts. Furthermore, the two asymmetries measured, one for the S1-S2 system and one for the S1-S3 system, were combined in geometric average to further reduce spurious asymmetries.

The polarization vector of the incident proton beam at the target was oriented along the + or $-\hat{x}$ direction for the determination of $K_x^{x'}(\theta)$, along the + or $-\hat{z}$ direction for $K_z^{x'}(\theta)$, and along the $+\hat{y}$ direction for $K_y^y(\theta)$ and $A(\theta)$. In the measurement of $P(\theta)$, the protons were unpolarized.

IV. DATA REDUCTION

The experimentally measured asymmetries were increased by multiplicative factors f, g, and h for background, multiple-scattering, and finite-geometry corrections, respectively. The latter two factors were functions chiefly of the neutron's energy, whereas f varied with the incident beam energy and the neutron production angle. The values used for these other factors are given in Fig. 2, and are discussed below.

All the correction factors were determined after the experimental spectrum had been well described by a Monte Carlo simulation of the experiment. The simulation was done with a Los Alamos Scientific Laboratory code[14] modified to include the experimental resolution which was treated as a folding function. In addition, consideration was given to the fact that the light output of the helium scintillator was not directly proportional to the

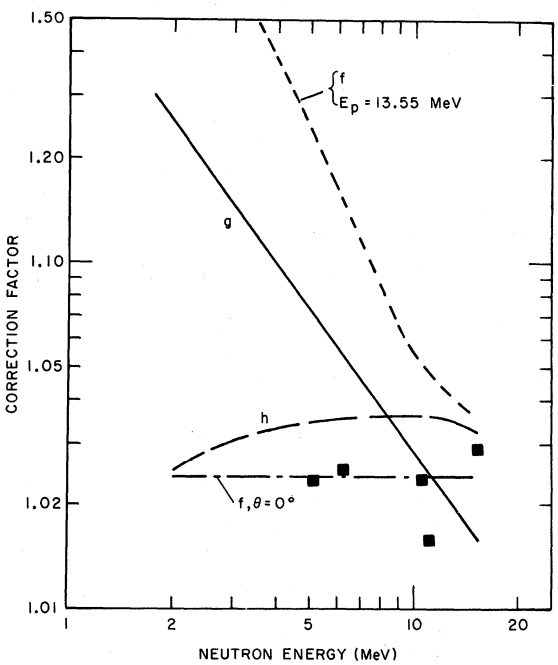

FIG. 2. Smoothed representations of correction factors for background (f), multiple scattering (g), and finite geometry (h). The squares represent 0° backgrounds.

α-recoil energy. In particular, one α recoil with energy E_α gave more light than two α recoils each with energy $\frac{1}{2}E_\alpha$. The result was that the double-scattered events were shifted to lower pulse heights relative to the single-scattered events and the triple relative to the double. For ease of calculation, the entire spectrum of double-scattered events was shifted by a constant value relative to the single-scattered events and the entire triple-scattered spectrum by the same value relative to the double. This procedure is exact if the light output of the scintillator is linear with α-recoil energy, that is, $L = aE_\alpha - b$. The constant b is then the amount of the shift and in practice was taken from a linear approximation to the response function of S1. This procedure gives an overestimate of the shift; however, it is believed that an improvement in the simulation of the experimental spectrum was obtained in this way.

Backgrounds were drawn in by hand as in Ref. 13 after the spectrum had been well fitted by the Monte Carlo calculation. An uncertainty of $\Delta f = \pm\frac{2}{3}(f-1)$ was ascribed to the background correction and became a significant uncertainty in the measurements at angles greater than 60°. The largest value of f was 1.4 at $\theta = 120°$. Target-empty runs indicated the background to be unpolarized. An additional background of unknown origin not observed in the target-empty runs was also assumed to be unpolarized.

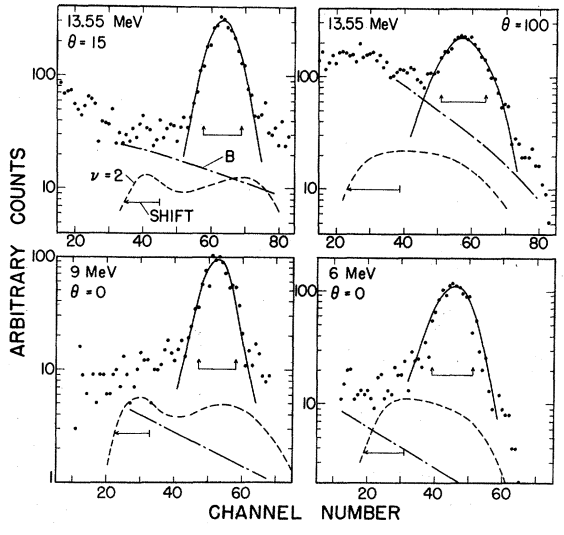

FIG. 3. Typical α-recoil pulse-height distributions. Each panel is labeled by the incident proton energy and lab angle. The bracketed interval of the peak represents the signal region. The dot-dash curve represents the estimate of background, while the dashed curve represents the doubly scattered ($\nu = 2$) events from a Monte Carlo calculation, shifted to lower channel number as described in the text.

The multiple-scattering correction factor, g, was taken from the Monte Carlo simulation. In view of the uncertainties in the shifting procedure, primarily, an uncertainty of $\Delta g = \pm\frac{1}{3}(g-1)$ was ascribed to this factor. In all cases the statistical uncertainty in g was less than Δg. The finite-geometry correction factor h was taken from the single-scattered events in the Monte Carlo simulation.

In Fig. 3 four representative spectra are given to illustrate the quality of the data, the Monte Carlo description of it, and the assumed background. The spectrum at 100° at 13.55 MeV corresponds very nearly to the same neutron energy as the 0° spectrum at 6 MeV. The much higher background of the former arises primarily from neutrons produced in the metal of the target.

To improve the ratio of these events to background and to minimize the multiple-scattering corrections, the asymmetries were calculated for that part of the peak which was approximately within the full width at half maximum as denoted by the arrows in Fig. 3. These asymmetries agreed with ones calculated from the full peaks when the appropriate correction factors were applied for background and multiple scattering. Thus we have confidence in our correction factors at least to the accuracy quoted.

The components of neutron polarization were extracted from the corrected asymmetries according to Eq. (10), using values of $P(n\text{-}\alpha, 115°)$ calculated from Satchler *et al.*[15] Finally, polarization transfer coefficients were calculated from these components and from the beam polarization according to Eqs. (1)–(4).

V. RESULTS AND DISCUSSION

A. Data at $E_p = 13.55$ MeV

The experimental values of the polarization function and the transfer functions are given in Table I. The values of $A(\theta)$ needed to calculate K_y^y were taken from an independent experiment to be reported elsewhere.[16] The errors are standard deviations and include statistical uncertainties as well as uncertainties in the correction factors. The uncertainty in the beam polarization, where appropriate, is not included; we estimate ±1.5% error from this cause as systematic error. Likewise, uncertainty in the n-He analyzing power is not included.

Figure 4 shows a comparison of our results for $P(\theta)$ at 13.55 MeV (closed circles) with experimental data of two other groups at nearby energies. The open triangles show the data of Walter *et al.*[17] at 12 MeV; the agreement is quite reasonable. Also shown are the published data of Alek-

seev *et al.*[18] at 12.2 and 14.5 MeV as open squares and diamonds, respectively. The experimental method of both groups was based on a high-pressure helium-gas scintillator with precession solenoid. At 15° the data of Ref. 18 have significantly smaller values than ours; otherwise the comparison is satisfactory. In fact, all the data are reasonably consistent, and indicate that the polarization function varies slowly with energy in this region. Also shown in Fig. 4 are theoretical curves from the formulation of WM. The curves reproduce the qualitative nature of the data, but lack quantitative agreement. We return to this comparison below.

In Fig. 5 are shown the experimental results for the polarization-transfer parameters K_y^y, $K_x^{x'}$, and $K_z^{x'}$ as functions of θ at 13.55 MeV. In this case, there are no other data with which to compare. There are some geometrical considerations that bear mentioning. If the process were pure p-n charge exchange in the absence of spin interaction, the neutron might be expected to retain the spin polarization of the incoming proton. Our measurements at 0° show that this is not true, since at this energy $K_y^y \approx 0.52$, which however, is not a small value. K_y^y is approximately constant out to 30°, but goes down significantly at 45°. Under the supposition above, $K_x^{x'}$ and $K_z^{x'}$ would represent the geometrical components of initial polarization proportional to $\cos\theta$ and $-\sin\theta$, respectively. These components are shown in Fig. 5 multiplied by the factor 0.52. One observes that the expected geometrical behavior does persist out to ≈30°, where well-marked deviations begin to occur.

In Figs. 4 and 5 comparisons are made to R-matrix calculations[19] based on the charge-independent analysis of Werntz and Meyerhof (their two solutions are denoted as WMI and WMII). Their analysis used Legendre coefficients representing existing $T(p,n)^3$He differential-cross-section and polarization data to provide information on the $T=0$ states of ^{4}He, together with p-^{3}He phase-shift analyses from various sources as input concerning the $T=1$ levels. $T(p,n)^3$He polarization information was used up to $E_p = 12.2$ MeV, representing an excitation in the compound nucleus ^{4}He of 28.96 MeV. On this basis we would expect to see a reasonably good comparison with the $T(p,n)^3$He polarization data at 13.55 MeV, since $P(\theta)$ is not changing rapidly with energy. Figure 4 shows this comparison. The solutions WMI and WMII differ little from each other and give a qualitative account of the shape of the data. At forward angles the curves are about a factor of 2 low relative to the data. The deviation is not

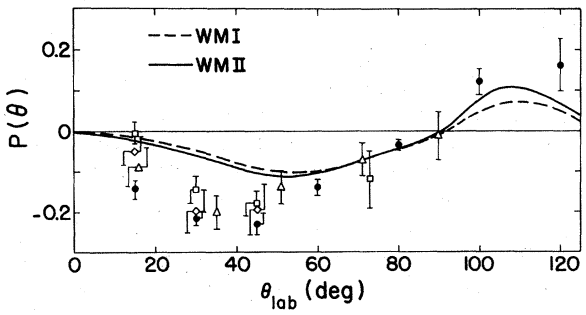

FIG. 4. $T(p,n)^3$He polarization data at 13.55 MeV and comparison with experiments at nearby energies. The experimental data are identified as follows: (●) this work; (△) Walter *et al.* (Ref. 17), 12.0 MeV; (□) Alekseev *et al.* (Ref. 18), 12.2 MeV; (◇) Alekseev *et al.* (Ref. 18), 14.5 MeV. The curves represent R-matrix calculations based on the Werntz and Meyerhof (WM) analysis.

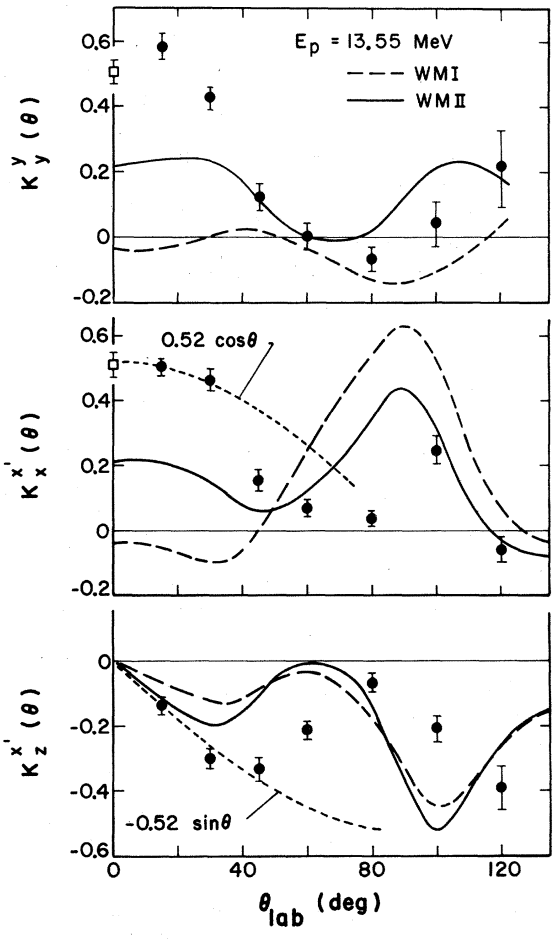

FIG. 5. $T(p,n)^3$He polarization-transfer data at 13.55 MeV for K_y^y (top panel), $K_x^{x'}$ (middle panel), and $K_z^{x'}$ (lower panel). The points at 0° (open squares) are interpolated from the 0° data of Table II. Also shown are R-matrix calculations based on the Werntz and Meyerhof (WM) analysis, and geometrical components.

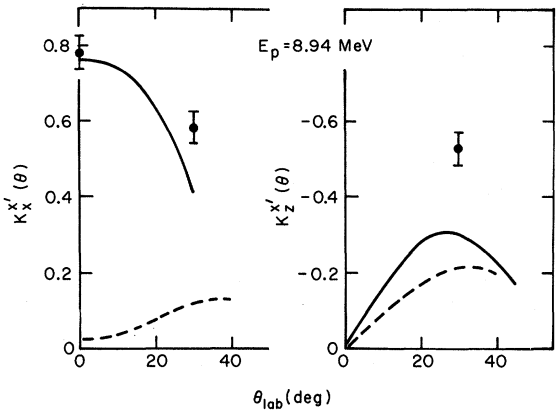

FIG. 6. Polarization-transfer data in the reaction $T(p,n)^3He$ at 8.94 MeV for $K_x^{x'}$ (left side) and $K_z^{x'}$ (right side). Comparisons with calculations based on the Werntz and Meyerhof (WM) analysis are also shown.

fully understood; presumably it indicates need for change in the WM level parameters.

Figure 5 shows the comparison between WM and the polarization-transfer functions. At forward angles the magnitudes of the predictions of WMI and WMII are less than experiment, although in every case WMII lies closer to the data. At backward angles the data show a tendency to form a peak; WMII reproduces this trend although generally shifted toward smaller angles. There is a discernible trend for WMII to reproduce qualitative features of the data, WMII more so than WMI. Quantitatively, the agreement is not good; however, it must be remembered that the comparisons being made here represent an extrapolation of ≈1.5 MeV above the range in which data were used by WM.

B. Data at E_p = 8.94 MeV

At the end of the runs at 13.55 MeV it was possible to obtain two data points at 8.94 MeV for $K_x^{x'}$ and $K_z^{x'}$ at 30°. These are given in Table I. They are also shown in Fig. 6 with additional data at 0° from K_y^y [$K_y^y(0°) = K_x^{x'}(0°)$], and compared with the WM predictions. In the case of $K_x^{x'}$ a large separation between the predictions for WMI and WMII occurs, with WMII being much closer to these small-angle data. In the case of $K_z^{x'}$ both predictions have values much smaller than that required by the single datum at 30°. This energy is well within the range covered by WM, and it may be that further effort on analysis and experiment at this energy would be profitable in understanding the ^{4}He problem.

C. Tabulation of Data on $K_y^y(0°)$

In Table II we document the data of our prior communication[1] on K_y^y at 0° as a function of energy. Given in the table is information on neutron energy, proton polarization, p_{iy}, measured asymmetry, e_M, measured neutron polarization, p_{fy}, as well as the final values of $K_y^y(0°)$. The background correction factor f was quite small for these data compared to results of large-angle measurements at E_p = 13.55 MeV of comparable neutron energy. This is illustrated in Figs. 2 and 3 where pulse-height distribution and correction factors are shown. These data were also compared earlier with the predictions of WMI and WMII to which we allude briefly here. At low energy, $3 \leq E_p \leq 6$ MeV, both solutions were in accord with the data. As the energy is increased both solutions show a more rapid energy variation than the data with

TABLE I. Polarization-transfer functions and the polarization function for the reaction $T(p,n)^3He$.

θ_{lab} (deg)	$K_x^{x'}(\theta)$	$K_z^{x'}(\theta)$	$K_y^y(\theta)$	$P(\theta)$
		E_p = 13.55 ± 0.05 MeV [a]		
15	+0.505 ± 0.026 [b]	−0.138 ± 0.025	+0.584 ± 0.039	−0.143 ± 0.023
30	+0.464 ± 0.031	−0.297 ± 0.028	+0.429 ± 0.034	−0.216 ± 0.017
45	+0.156 ± 0.033	−0.332 ± 0.033	+0.124 ± 0.042	−0.229 ± 0.027
60	+0.070 ± 0.026	−0.211 ± 0.026	+0.004 ± 0.037	−0.139 ± 0.021
80	+0.038 ± 0.021	−0.065 ± 0.028	−0.071 ± 0.040	−0.033 ± 0.014
100	+0.247 ± 0.042	−0.209 ± 0.039	+0.045 ± 0.066	+0.122 ± 0.031
120	−0.058 ± 0.041	−0.390 ± 0.068	+0.218 ± 0.123	+0.162 ± 0.064
		E_p = 8.95 ± 0.07 MeV		
30	+0.585 ± 0.042	−0.529 ± 0.042		

[a] The uncertainty in energy is the half energy loss in the tritium gas cell.

[b] Errors are standard deviations and include contributions from statistics, and correction factors from background, multiple scattering, and finite geometry. Not included are contributions from incident beam polarization or $P_{n\text{-He}}$.

WMI departing markedly from the data, and going negative in fact at $E_p = 9$ MeV. This behavior was thought to be significant chiefly in demonstrating a sensitivity to the level structure of ^{4}He, rather than allowing a choice between the solutions I and II.

D. Utility as a Source of Polarized Neutrons

The $T(p,n)^3$He reaction is a primary source of neutrons at low energies (1–10 MeV) owing to its high 0° cross section, especially in the lower part of this range, and its relative freedom from background neutrons. With an unpolarized proton beam incident, polarized neutrons may be obtained at angles of ≈35°, where the cross section is lower than at 0°. Walter[20] has reviewed this process as a polarized neutron source, and he notes that above $E_n = 3$ MeV the neutron polarization is relatively low, $P \approx 0.2$. The advent of polarized incident proton beams clearly allows polarized neutrons to be obtained by polarization transfer. The usefulness of this process depends on incident beam intensity; however, modern ion sources are capable of putting 50 to 100 nA on target. For polarization transfer at 0° the data of Table II show that neutron polarization in the neighborhood of 0.6 or greater can be obtained for neutron energies in the range of 2 to 10 MeV. Since the relevant comparison is $P^2(\theta)I(\theta)$, the increase in P^2 with some advantage from $I(0°)/I(35°)$ implies that the polarized beam may be $\frac{1}{10}$ as intense as the unpolarized beam and be competitive as a source of polarized neutrons.

Finally we note that by using the polarization-transfer process at a nonzero angle, it is possible to increase the polarization of the outgoing neutrons by arranging constructive signs of the terms $P(\theta)$ and $K_y^y(\theta)$ of Eq. (2). For example, at $E_p = 13.55$ MeV and 15° lab with $p_{iy} = -1.0$, $p_{fy} = 0.661 \pm 0.045$; the figure of merit for producing polarized neutrons for these conditions is approximately a factor of 1.3 higher as compared to 0°. Similar considerations will also hold at lower energies, although the pertinent measurements of $K_y^y(\theta \neq 0°)$ have not yet been made.

VI. CONCLUSION

In conclusion, these measurements have revealed large effects in the polarization-transfer process for the reaction $T(p,n)^3$He. At 13.55 MeV and at small angles, the effects are consistent with a naïve picture of charge-exchange scattering in which the outgoing neutron retains part of the incoming spin polarization. Predictions for the polarization-transfer parameters from the formulation of Werntz and Meyerhof have reproduced qualitative aspects of the data; quantitative agreement is lacking. The consequence is that changes will be necessary in the present knowledge of states of ^{4}He in order to accommodate the present data.

TABLE II. Polarization-transfer function, $K_y^y(0°)$, in the reaction $T(p,n)^3$He versus proton energy.

$E_p \pm \frac{1}{2}\Delta E_p$ [a]	E_n	p_{iy}	e_M [b]	P_{fy}	$K_y^y(0°)$
2.90 ± 0.17	2.12	0.885	0.356 ± 0.012 [c]	0.559 ± 0.042	0.632 ± 0.048
3.90 ± 0.13	3.12	0.896	0.471 ± 0.013 [c]	0.592 ± 0.030	0.661 ± 0.033
4.92 ± 0.11	4.15	0.898	0.540 ± 0.034	0.646 ± 0.047	0.719 ± 0.052
5.43 ± 0.10	4.66	0.902	0.521 ± 0.018	0.614 ± 0.028	0.681 ± 0.031
5.93 ± 0.09	5.16	0.898	0.598 ± 0.029	0.650 ± 0.032	0.724 ± 0.036
6.44 ± 0.09	5.67	0.901	0.615 ± 0.023	0.710 ± 0.033	0.788 ± 0.037
6.94 ± 0.08	6.17	0.895	0.683 ± 0.036	0.742 ± 0.040	0.828 ± 0.045
7.44 ± 0.08	6.67	0.890	0.633 ± 0.028	0.720 ± 0.036	0.808 ± 0.040
7.94 ± 0.07	7.17	0.888	0.621 ± 0.033	0.701 ± 0.042	0.789 ± 0.047
8.45 ± 0.07	7.68	0.898	0.614 ± 0.036	0.691 ± 0.043	0.769 ± 0.048
8.95 ± 0.07	8.18	0.882	0.642 ± 0.034	0.692 ± 0.038	0.785 ± 0.043
9.95 ± 0.06	9.18	0.888	0.537 ± 0.038	0.595 ± 0.044	0.670 ± 0.050
10.96 ± 0.05	10.19	0.881	0.560 ± 0.037	0.600 ± 0.042	0.681 ± 0.048
11.95 ± 0.05	11.18	0.898	0.477 ± 0.036	0.509 ± 0.039	0.567 ± 0.043
12.95 ± 0.05	12.18	0.906	0.455 ± 0.045	0.499 ± 0.051	0.551 ± 0.056
13.95 ± 0.05	13.18	0.915	0.370 ± 0.037	0.406 ± 0.042	0.444 ± 0.046
14.96 ± 0.04	14.19	0.910	0.428 ± 0.033	0.463 ± 0.036	0.509 ± 0.039
15.96 ± 0.04	15.19	0.911	0.327 ± 0.030	0.358 ± 0.033	0.393 ± 0.036

[a] $\frac{1}{2}\Delta E_p$ is the half energy loss in the tritium gas cell.

[b] The measured asymmetry e_M is related to the corrected asymmetry e by $e = fgh e_M$, where f, g, and h are correction factors given in the text. Errors are standard deviations, and include contributions from the correction factors, but not p_{iy} or $P_{n\text{-He}}$.

[c] Average of runs on different days.

ACKNOWLEDGMENTS

We wish to thank John Martin for invaluable assistance with the experiment. We are indebted to Dr. G. P. Lawrence and Dr. J. L. McKibben for providing the intense polarized proton beam from the ion source, and to Dr. R. L. Henkel and the tandem-accelerator staff for their excellent cooperation. Many useful conversations with Dr. G. M. Hale are gratefully acknowledged.

APPENDIX A

The form of the Wolfenstein equations for the polarization-transfer functions, $K^{\mu}_{\omega}(\theta)$, may be written in a general way as follows:

$$I(\theta)p_{f\mu} = I_0(\theta)[P_{\mu}(\theta) + \sum_{\omega=x,y,z} \vec{p}_i \cdot \hat{\omega} K^{\mu}_{\omega}(\theta)], \qquad \text{(A1)}$$

where $I(\theta)$ and $I_0(\theta)$ are the polarized and unpolarized differential cross sections, with $P_{\mu}(\theta)$ being assumed polarization functions. The label μ ranges over $\hat{x}'$, $\hat{y}'$, or $\hat{z}'$ in the final laboratory frame of reference; x, y, z refer to the incident laboratory frame. The pseudovector $\vec{p}_f$ is constructed by multiplying each component given above by the appropriate unit vector $\hat{x}'$, $\hat{y}$, or $\hat{z}'$. The initial polarization, $\vec{p}_i$, is also a pseudovector, which implies that $\vec{p}_i \cdot \hat{y}$ is a scalar, whereas $\vec{p}_i \cdot \hat{x}$ and $\vec{p}_i \cdot \hat{z}$ are pseudoscalars. The functions $P_{\mu}(\theta)$ and $K^{\mu}_{\omega}(\theta)$ are considered to be scalars. To maintain the pseudovector nature of $\vec{p}_f$ we require P_x, P_z, K^{y}_{x}, $K^{x'}_{y}$, $K^{z'}_{y}$, and K^{y}_{z} all to be zero, which establishes the form of Eqs. (1)–(3).

In a similar fashion $I(\theta)$ may be written in a general way,

$$I(\theta) = I_0(\theta)[1 + \sum_{\omega=x,y,z} \vec{p}_i \cdot \hat{\omega} A_{\omega}(\theta)]. \qquad \text{(A2)}$$

$I(\theta)$ must be a scalar. Thus, terms involving $\vec{p}_i \cdot \hat{x}$ and $\vec{p}_i \cdot \hat{z}$ must vanish, i.e., $A_x = A_z = 0$, and the form of Eq. (4) is established. To simplify notation we drop the y subscript for the polarization function and analyzing power and use $P(\theta)$ and $A(\theta)$ where they occur.

APPENDIX B

In two-body scattering or reactions the M matrix relates final spin states to initial ones. The reaction $T(p, n)^3He$ is very similar to the N-N system, but restricted only by rotation and space-reflection invariance. MacGregor, Moravcsik, and Stapp[10] have given a general form of M which applies to our case, namely, in our notation,

$$\begin{aligned} M = {} & a + b(\vec{\sigma}_1 \cdot \hat{y} - \vec{\sigma}_2 \cdot \hat{y}) + c(\vec{\sigma}_1 \cdot \hat{y} + \vec{\sigma}_2 \cdot \hat{y}) + m(\vec{\sigma}_1 \cdot \hat{y}\, \vec{\sigma}_2 \cdot \hat{y}) \\ & + g(\vec{\sigma}_1 \cdot \hat{z}'\, \vec{\sigma}_2 \cdot \hat{z}' + \vec{\sigma}_1 \cdot \hat{x}'\, \vec{\sigma}_2 \cdot \hat{x}') \\ & + h(\vec{\sigma}_1 \cdot \hat{z}'\, \vec{\sigma}_2 \cdot \hat{z}' - \vec{\sigma}_1 \cdot \hat{x}'\, \vec{\sigma}_2 \cdot \hat{x}') \\ & + t(\vec{\sigma}_1 \cdot \hat{x}'\, \vec{\sigma}_2 \cdot \hat{z}') + t'(\vec{\sigma}_1 \cdot \hat{z}'\, \vec{\sigma}_2 \cdot \hat{x}'). \end{aligned} \qquad \text{(B1)}$$

The coefficients $a, b, \ldots, t'$ may be considered scalar functions of the c.m. angle and energy, whereas the coordinate system defining the components of the Pauli spin operators is the final laboratory system x', y', z'. This situation is the same for the N-N problem where the usual unit vectors $\hat{K}$, $\hat{N}$, $\hat{P}$ also define a final laboratory frame of reference. The unit vectors $\hat{x}'$, $\hat{y}'$, $\hat{z}'$ could be expressed in the final c.m. frame by a rotation of coordinates by the difference between the c.m. and laboratory angles. In Eq. (B1) above, the subscript (1) denotes the nucleon, while the subscript (2) denotes the mass-3 particle, with the assumption that suitable charge-exchange operators change the incident proton to the final neutron, and similarly for the mass-3 particle.

The M matrix for the N-N problem also has this form except that $b = 0$ owing to the identity of the particles or the related consequence of charge independence, as explained in standard texts.[21] Another feature of the N-N problem is that, for nonrelativistic scattering, the laboratory scattering angle is half the c.m. scattering angle. Hence the final laboratory z' direction is along $\vec{k}_{in} + \vec{k}_{out}$ with the momentum wave vectors defined in the c.m. system. Invariance arguments based on time reversal[22] show that t and t' are identically zero in this x', y', z' coordinate system. If the coordinate system is rotated about the y' axis, the form of M is the same, but the coefficients h, t, and t' transform among themselves linearly and, in general, t and t' are not zero.

APPENDIX C

The observables are related to the M matrix by the density-matrix formalism.[21] The initial density matrix for a polarized proton beam is $\rho_i = \frac{1}{4}(I_1 + \vec{p}_{1i} \cdot \vec{\sigma}_1) I_2$, where I_1 and I_2 represent unit matrices for particles 1 and 2. The final normalized density matrix is $\rho_f = (M\rho_i M^{\dagger})/\mathrm{Tr}(M\rho_i M^{\dagger})$. The expected value of the final spin polarization for the outgoing neutron is $\langle \vec{\sigma}_1 \rangle_f = \vec{p}_{1f} = \mathrm{Tr}(M\rho_i M^{\dagger} \vec{\sigma}_{1f})/(\mathrm{Tr} M\rho_i M^{\dagger})$. Note that all operators and vectors must be expressed in the same coordinate system, which in our case is the final laboratory frame, $\hat{x}'$, $\hat{y}$, $\hat{z}'$. For example, if the incident polarization is $\vec{p}_i = p_{ix}\hat{x}$, its resolution in the final laboratory system is $p_{ix}(\hat{x}' \cos\theta + \hat{z}' \sin\theta)$,

as used in Eq. (6).

Applying these rules, we write down the relations between the polarization-transfer observables and the coefficients of the M matrix, and for $I_0(\theta)$, $P(\theta)$, and $A(\theta)$ as well:

$$I_0(\theta) = |a|^2 + 2|b|^2 + 2|c|^2 + |m|^2 + 2|g|^2 + 2|h|^2 + |t|^2 + |t'|^2, \quad \text{(C1)}$$

$$I_0(\theta)P(\theta) = 2\mathrm{Re}[a(b^* + c^*) + m^*(c - b)] - 2\mathrm{Im}[t'(g^* - h^*) + t^*(g + h)], \quad \text{(C2)}$$

$$I_0(\theta)A(\theta) = 2\mathrm{Re}[a(b^* + c^*) + m^*(c - b)] + 2\mathrm{Im}[t'(g^* - h^*) + t^*(g + h)], \quad \text{(C3)}$$

$$I_0(\theta)K_y^y(\theta) = |a|^2 + 2|b|^2 + 2|c|^2 + |m|^2 - 2|g|^2 - 2|h|^2 - |t|^2 - |t'|^2, \quad \text{(C4)}$$

$$K_x^{x'}(\theta) = \cos\theta K_{x'}^{x'}(\theta) + \sin\theta K_{z'}^{x'}(\theta), \quad \text{(C5)}$$

$$K_z^{x'}(\theta) = -\sin\theta K_{x'}^{x'}(\theta) + \cos\theta K_{z'}^{x'}(\theta), \quad \text{(C6)}$$

$$K_x^{z'}(\theta) = \cos\theta K_{x'}^{z'}(\theta) + \sin\theta K_{z'}^{z'}(\theta), \quad \text{(C7)}$$

$$K_z^{z'}(\theta) = -\sin\theta K_{x'}^{z'}(\theta) + \cos\theta K_{z'}^{z'}(\theta), \quad \text{(C8)}$$

where

$$I_0(\theta)K_{x'}^{x'}(\theta) = |a|^2 - |m|^2 + |t|^2 - |t'|^2 - 4\mathrm{Re}(bc^* + gh^*), \quad \text{(C9)}$$

$$I_0(\theta)K_{z'}^{z'}(\theta) = |a|^2 - |m|^2 - |t|^2 + |t'|^2 - 4\mathrm{Re}(bc^* - gh^*), \quad \text{(C10)}$$

$$I_0(\theta)K_{x'}^{z'}(\theta) = 2\mathrm{Re}[t(g^* + h^*) + t'(g^* - h^*)] - 2\mathrm{Im}[a(b^* + c^*) + m^*(c - b)], \quad \text{(C11)}$$

and

$$I_0(\theta)K_{z'}^{x'}(\theta) = 2\mathrm{Re}[t(g^* + h^*) + t'(g^* - h^*)] + 2\mathrm{Im}[a(b^* + c^*) + m^*(c - b)]. \quad \text{(C12)}$$

It may be noted that $P(\theta) \neq A(\theta)$ explicitly in the expressions above. For elastic scattering, i.e., T(p,p)T, the quantity $t'(g^* - h^*) + t^*(g + h)$ is in general nonzero, since the laboratory scattering angle is, in general, not half of the c.m. angle (see Appendix B). However, the quantity can be shown to be purely real owing to time-reversal invariance. Hence for elastic scattering, $P(\theta) = A(\theta)$, which is a well-known result from general symmetry conditions.[23]

†Work performed under the auspices of the U. S. Atomic Energy Commission.

*Visiting staff member to the Los Alamos Scientific Laboratory.

[1]T. R. Donoghue, R. C. Haight, G. P. Lawrence, J. E. Simmons, D. C. Dodder, and G. M. Hale, Phys. Rev. Letters 27, 947 (1971).

[2]C. Werntz and W. E. Meyerhof, Nucl. Phys. A121, 38 (1968).

[3]D. C. Dodder and G. M. Hale, private communication.

[4]J. L. Detch, Jr., R. L. Hutson, N. Jarmie, and J. H. Jett, Phys. Rev. C 4, 52 (1971).

[5]L. P. Robertson, R. C. Hanna, K. Ramavataram, D. W. Devins, T. A. Hodges, Z. J. Moroz, S. J. Hoey, and D. J. Plummer, Nucl. Phys. A134, 545 (1969).

[6]L. Wolfenstein, Ann. Rev. Nucl. Sci. 6, 43 (1956).

[7]Unless otherwise stated, angular measure or the symbol θ refers to laboratory scattering angles throughout the paper.

[8]C. R. Schumacher and H. A. Bethe, Phys. Rev. 121, 1534 (1961).

[9]*Proceedings of the Third International Symposium on Polarization Phenomena in Nuclear Reactions, Madison, 1970,* edited by H. H. Barschall and W. Haeberli (University of Wisconsin Press, Madison, 1971) p. xxv.

[10]M. H. MacGregor, M. J. Moravcsik, and H. P. Stapp, Ann. Rev. Nucl. Sci. 10, 291 (1960).

[11]G. P. Lawrence, G. G. Ohlsen, and J. L. McKibben, Phys. Letters 28B, 594 (1969).

[12]G. G. Ohlsen, J. L. McKibben, G. P. Lawrence, P. W. Keaton, Jr., and D. D. Armstrong, Phys. Rev. Letters 27, 599 (1971).

[13]G. S. Mutchler, W. B. Broste, and J. E. Simmons, Phys. Rev. C 3, 1031 (1971).

[14]J. E. Simmons, K. R. Crandall, and R. B. Perkins, unpublished.

[15]G. R. Satchler, L. W. Owen, A. J. Elwyn, G. L. Morgan, and R. L. Walter, Nucl. Phys. A112, 1 (1968).

[16]J. J. Jarmer, J. C. Martin, R. C. Haight, J. E. Simmons, and T. R. Donoghue, unpublished.

[17]R. L. Walter, W. Benenson, P. S. Dubbeldam, and T. H. May, Nucl. Phys. 30, 292 (1962).

[18]N. V. Alekseev, U. R. Arifkhanov, N. A. Vlasov, V. V. Davydov, and L. N. Samoilov, Zh. Eksperim. i Teor. Fiz. 45, 1416 (1963) [transl.: Soviet Phys.–JETP 18, 979 (1964)].

[19]We are indebted to G. M. Hale and D. C. Dodder for these calculations.

[20]R. L. Walter, in *Proceedings of the International Symposium on Polarization Phenomena in Nuclear Reactions, Madison, Wisconsin, 1970* (see Ref. 9).

[21]M. L. Goldberger and K. M. Watson, *Collision Theory* (Wiley, New York, 1964).

[22]L. Wolfenstein and J. Ashkin, Phys. Rev. 85, 947 (1952).

[23]A. Bohr and B. R. Mottelson, *Nuclear Structure* (Benjamin, New York, 1969), pp. 29–31.